CMS Physics Analysis Summary

Contact: cms-pag-conveners-higgs@cern.ch 2012/07/06

Search for SuperSymmetric Higgs boson states decaying into $b\bar{b}$ and produced in association with b-quarks in events collected by semi-leptonic triggers in pp collisions at $\sqrt{s} = 7$TeV

The CMS Collaboration

Abstract

This paper presents a search of neutral Supersymmetric Higgs particles produced in association with two spectator b-quarks and decaying to pairs of b-quarks. The data used correspond to 4.8 fb^{-1} collected by the CMS experiment at the LHC during the 2011 run, at a center of mass energy of 7 TeV. The data passed a semi-leptonic trigger that required a muon in the final state. Two different data driven methods to predict the background are described, yielding low statistical and systematic uncertainties. The results are presented in the framework of MSSM, in the m_h^{max} scenario.

1 Introduction

The electroweak symmetry breaking mechanism of the Standard Model (SM) predicts the existence of a neutral scalar boson, the Higgs particle, currently constrained by experimental observations to be in the mass range $115 - 128\,\mathrm{GeV}/c^2$ [1, 2]. In the SM framework the calculation of the mass of the Higgs boson diverges due to radiative corrections at high energies. Supersymmetry provides a solution to this problem, by introducing Super-partners of SM particles that cause suitable cancellations of divergent contributions.

In the Minimal Supersymmetric Standard Model (MSSM) [3] there are two Higgs doublets, which lead to five physical Higgs states: two neutral CP-even particles (h,H), one neutral pseudo-scalar (A) and a pair of charged states ($H^{\pm}$). Recent CMS results in $h/A \rightarrow \tau\tau$ decay mode [4] put severe constraints on the mass of the neutral states, significantly improving previous results by LEP [5] and Tevatron [6] experiments. Higgs particles decay mainly to pairs of b-quarks in the SM and for a large range of MSSM parameter space. However, huge QCD backgrounds make this mode particularly difficult for the SM searches. For the MSSM searches the possibility exists of observing the additional b-quarks produced in association with the MSSM Higgs, which allow to reduce the QCD background significantly as shown by recent publications by CDF and D0 [7, 8].

This PAS note introduces a search for MSSM neutral Higgs states decaying into a pair of b-quarks, performed on the data collected in 2011 by CMS using dedicated triggers based on the detection of moderately high transverse momentum p_{T}, non-isolated muons and two jets with on-line b-tagging. The use of a muon and jet triggered dataset allows us to tag the semi-muonic decay of one of the b-quarks. A dataset with a muon in the trigger can also tolerate lower energy thresholds on jets in the trigger, improving the overall sensitivity. A parallel analysis, using a full hadronic trigger, has also been presented by CMS [9].

2 Detector description and reconstruction

The data sample used in this search corresponds to an integrated luminosity of $4.8\,\mathrm{fb}^{-1}$ recorded in 2011 with the CMS detector at the LHC, running at a center-of-mass energy of 7 TeV.

The central feature of the Compact Muon Solenoid (CMS) apparatus is a superconducting solenoid of 6 m internal diameter, providing a magnetic field of 3.8 T. Within the field volume, the inner tracker is formed by a silicon pixel and strip tracker. It measures charged particles within the pseudorapidity range $|\eta| < 2.5$. It provides an impact parameter resolution of $\sim$15 μm and a p_{T} resolution of about 1.5% for 100 GeV/c particles. Still inside the field volume are a crystal electromagnetic calorimeter (ECAL) and a brass/scintillator hadron calorimeter (HCAL). Muons are measured in gas-ionization detectors embedded in the steel return yoke. Muons are measured in the pseudorapidity range $|\eta| < 2.4$, with detection planes made using three technologies: drift tubes, cathode strip chambers, and resistive plate chambers. Matching muons to tracks measured in the silicon tracker (global muons) results in a transverse momentum resolution between 1 and 5%, for p_{T} values up to 1 TeV/c. Extensive forward calorimetry complements the coverage provided by the barrel and endcap detectors.

A more detailed description of the CMS detector can be found in Ref. [10].

In this analysis, a particle-flow (PF) event reconstruction [11] is used. It reconstructs and identifies each particle with an optimised combination of all subdetector information. Photons and electrons are reconstructed using ECAL and inner tracker. The energy of muons is obtained from the corresponding track momentum. The energy of charged hadrons is determined from

a combination of the track momentum and the corresponding ECAL and HCAL energy, corrected for zero-suppression effects, and calibrated for the nonlinear response of the calorimeters. Finally the energy of neutral hadrons is obtained from the corresponding calibrated ECAL and HCAL energy.

Jets are reconstructed offline from the reconstructed particles, clustered by the anti-k_t algorithm [12] with a size parameter of 0.5. Jet momentum is determined as the vector sum of all particle momenta in the jet, and is found by simulation to be on average within 5% to 10% of the true momentum over the whole p_T spectrum and detector acceptance. An offset correction is applied to take into account the extra energy clustered in jets due to additional proton-proton interactions within the same bunch crossing. Jet energy corrections are derived from the simulation, and are confirmed with in situ measurements with the energy balance of dijet and photon+jet events. The jet b-tagging algorithm used is the Combined Secondary Vertex (CSV) [13], which combines in a likelihood ratio information about impact parameter significance, the secondary vertex and jet kinematics.

3 Signal characterization

Simulations of neutral MSSM Higgs decaying to b-quarks show that the highest energy b-jets in the events originate from the Higgs decay. This happens for 80% of the events at $m_H = 120\,\text{GeV}/c^2$. For 67% of these decays Higgs decays, the PF algorithm successfully reconstructs two jets with $p_T \geq 30\,\text{GeV}/c$. These numbers increase for higher Higgs mass values. The dynamic of the production is such that quite frequently the fourth b-quark jet is outside the central region ($|\eta| < 2.5$) and often is so far forward that it escapes detection altogether. The b-jets not originating from the Higgs decay have a considerably softer p_T spectrum. In addition, the muons originating from these spectator b-quark decay are softer than muons from the Higgs decay chain. For a signal sample of $m_H = 120\,\text{GeV}/c^2$, 20% of the events contain a reconstructed muon with $p_T \geq 5\,\text{GeV}/c$. With a harder muon, at $p_T \geq 12$, 15 or 17 GeV/c, the fraction of events that satisfies the requirement falls to 7%, 4.5% or 3.5% respectively.

After the trigger selection requirements (described in more detail below), the overall efficiency on the signal including the semileptonic branching fraction of the b decay is approximately 2% for $m_H = 120\,\text{GeV}/c^2$, increasing to 9% for $m_H = 250\,\text{GeV}/c^2$. These values differ slightly for the different data taking periods in which different High Level Triggers (HLT) paths were used. The typical mass resolution on the reconstructed Higgs invariant mass is about 15% .

4 Trigger and event selection

The data used in the analysis have been collected during 2011, using five different HLT trigger paths. All the triggers required a muon above $p_T = 12\,\text{GeV}/c$ threshold and the presence of one or two central jets ($|\eta| < 2.6$) with transverse energy above a given threshold (20 or 30 GeV/c, depending on the data taking period), with at least one or two on-line b-tagged jets.

The offline analysis requirements at pre-selection stage are the following:

- One good primary vertex;
- A global muon with $p_T > 15\,\text{GeV}/c$, no explicit isolation required;
- At least three jets within $|\eta| < 2.6$ and with transverse energy $E_T > 30\,\text{GeV}$ for the first two and $E_T > 20\,\text{GeV}$ for the third and following ones;
- The separation between any pair of jets has to be $\Delta R_{ij} > 1$ in order to avoid any

ambiguities in b-tagging;

- The first two jets, ordered in E_T, have to have CSV b-tag discriminator value $CSV > 0.8$;
- The global muon has to be used in the reconstruction of one of the two leading jets.

The final selection for the signal search adds the requirement for the third jet to have a CSV b-tag value greater than 0.7.

The data reduction after each cut, as well as the total integrated luminosity collected with all relevant triggers, is shown in Tab. 1,

Table 1: Data reduction after each selection cut.

Cut	Events
All	16732273
$p_{\mathrm{T}}^{\mu} > 15\,\mathrm{GeV}/c$	9739139
$\#jets >= 3$	4511327
$\Delta R_{ij} >= 1$	3505584
$CSV(1^{st} - jet) > 0.8$	1932135
$CSV(2^{nd} - jet) > 0.8$	813685
μ in 1^{st} or 2^{nd} jet	785940
$CSV(3^{rd} - jet) > 0.7$	60195
$\int \mathcal{L}dt\ [\mathrm{pb}^{-1}]$	4805.7

The relative efficiency of the muon triggers with respect to the off-line selection criteria were measured using pre-scaled low threshold single muon triggers. A value of about $45 - 60\%$ was found, depending to the Higgs mass.

5 Background determination

The relevant background processes for this analysis are studied using simulated events, produced for $t\bar{t}$ by the MADGRAPH [14] Monte Carlo (MC) generator and with PYTHIA [15] for the other processes. The $Z \to b\bar{b}$ yield is rescaled to match the MADGRAPH jets multiplicity. All simulated datasets are then processed using GEANT4 [16] with a detailed CMS detector simulation, including the PileUp events as observed during 2011 data taking, and finally reconstructed with the same reconstruction program used for data. The expected events for each process are shown in Tab. 2: each process is normalized using the measured cross section to the total integrated luminosity used, with the exception of multijet QCD background, for which the nominal PYTHIA cross section has been used.

The major background for the Higgs decaying to b-quarks comes from multijet events from hard scattering QCD processes. For these process, MC simulation is not feasible due to the uncertainties of multiple b-jet production in gluon splitting, as well as the lack of NLO/NNLO cross section. Other background processes such as $t\bar{t}$ + jets, $Z \to b\bar{b}$ + jets, are predicted to be at the percent level or less of the total background by the MC simulation. These backgrounds are minor compared to the overwhelming multijet QCD background, and that are taken into account in a data-driven background evaluation procedure described below.

Two independent methods were developed to predict the expected background. The first is a data-driven method based on the computation of b-tagging matrices using templates, and the

Table 2: Events passing all analysis cuts for MC simulated background samples. The quoted errors are statistical only.

Process	events
Multijet QCD	72043±747
$t\bar{t}$ + jets	303±5.8
$Z \to b\bar{b}$	540±70
ZZ	1.84±0.07
WZ	0.44±0.05
WW	0.03±0.03

second one is based on a nearest-neighbor in parameter-space technique called Hyperball. The former is used for the predicted background, and the latter to assess the systematics uncertainties in this prediction.

In order to find a background-enhanced, signal-depleted control region, a likelihood discriminating variable is constructed (*Discr*) with various kinematic inputs (such as p_T of the b-jets, separation in ϕ and η of the b-jets, separation in ϕ, η between the third jet and the combination of the two leading, b-jet multiplicity). Two versions of this discriminator are used: one for the low mass Higgs region ($m_H \leq 180\,\text{GeV}/c^2$) and another for the high mass Higgs ($m_H > 180\,\text{GeV}/c^2$). The distributions of *Discr* as defined for the low mass Higgs is shown for the MC multijet QCD background and for the Higgs signal in Fig. 1 as well as for other electroweak backgrounds: $t\bar{t} \to W^+bW^-\bar{b}$ and $Z \to b\bar{b}$. For both discriminators, the control region is defined as the sample of events having a value $Discr < 0.4$.

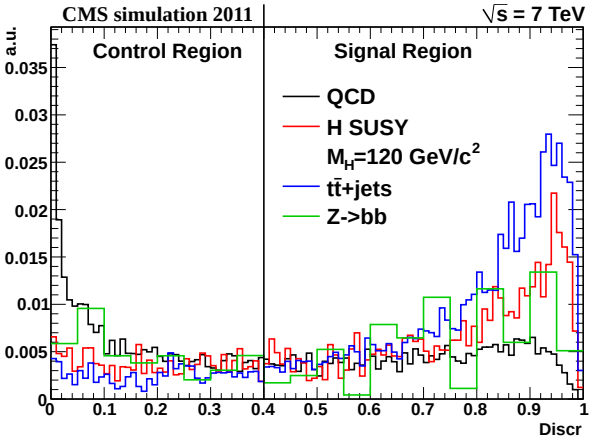

Figure 1: Distribution of the discriminating variable used for $M_H \leq 180\,\text{GeV}/c^2$ as defined in the text for multijet QCD background events (black), $t\bar{t}$ (blue), $Z \to b\bar{b}$ (green) and SUSY Higgs signal for $m_H = 120\,\text{GeV}/c^2$ (red). All distributions are normalized to unity. In the analysis, the multijet QCD background is the largest one by far, and $t\bar{t} \to W^+bW^-\bar{b}$ and $Z \to b\bar{b}$ are expected to be small, as shown in Tab. 2.

The *Discr* variable can be calculated for single b-jet (bjj) and double b-jet (bbj) events. Figure 1 includes the two most important electroweak backgrounds $t\bar{t}$+jets and $Z \to b\bar{b}$+jets. In particular, the $Z \to b\bar{b}$ resonant process has a *Discr* distribution different from signal.

The *Discr* distribution shows multijet QCD MC simulation, which as noted above is not expected to mimic the data faithfully. Therefore, it is not used to test the presence of a signal, but only to find a region of phase space where the multijet background is high compared to signal

in events with three b-tag.

The method based on the b-tagging matrices is described below: for any observable x, the prediction of its distribution $F(x;bbb)$ in the 3 b-jet sample can be computed as follows:

$$F(x;bbb) = F(x;bbj) \times P_{b-tag}^{3rd-j}(j) \tag{1}$$

where $P_{b-tag}^{3rd-j}(j)$ is the probability of the third jet to be b-tagged, according to the b-tagging algorithm and threshold used for the third jet. $F(x;bbj)$ is the observed distribution for the same observable x in the sample with three jets, where only the two highest E_T jets are b-tagged.

Taking into account the contribution of b, c, and light (uds-quarks plus gluon) jets $P_{b-tag}^{3rd-j}(j)$ expands as follows:

$$P_{b-tag}^{3rd-j}(j) = \epsilon_b \cdot f_b + \epsilon_c \cdot f_c + \epsilon_{light} \cdot (1 - f_b - f_c) \tag{2}$$

where ϵ_b, ϵ_c and ϵ_{light} are the probabilities for a b, c, or light jet to be b-tagged, respectively (or efficiency). The $f_{b,c}$ are the fractions of the corresponding quarks for the third jet in the events.

Efficiencies and quark fractions depend on the third jet kinematics as well as other event characteristics. The efficiencies are parametrized as a function of E_T, $|\eta|$ and charge multiplicity of the third jet. An additional two parameter function parametrizes the heavy flavour fraction:

$$f_{b,\,c,\,light} = f_1\left(E_t^{(3^{rd}\ jet)}, |\eta^{(3^{rd}\ jet)}|\right) \times\ f_2\left(\Delta R_{1,2}, \Delta R_{H,3}\right) \tag{3}$$

where the first term f_1 uses the same variables as the efficiency, and the second term f_2 uses two variables that describe the event topology: the angular separation between the first and the second b-jet $\Delta R_{1,2}$ and the angular separation between the third jet and the object resulting from the combination of the first and second jet (the Higgs candidate, denoted as H in the subscript). The second factor is used only for the shape of the distribution, it is normalized to unity, taking into account the event distribution in the $(\Delta R_{1,2}, \Delta R_{H,3})$ plane.

The ϵ_b, ϵ_c and ϵ_{light} efficiencies are taken from the MC simulation. A detailed study of the b-tagging efficiency described in [13] using several data driven methods, provides a scale factor for the efficiency as found from the MC with respect to data. For the CSV working point used for the third jet, the scale factor is 0.95 ± 0.04, and it is fairly independent on the b-jet p_{T} for the range considered in the present analysis. This scale factor is applied to the b-tagging efficiency. No additional bias has been observed for the particular cuts of this analysis.

The heavy flavour fractions are obtained from the data for each bin of the aforementioned parametrization planes. The observables used to fit the data are the invariant mass associated with the secondary vertex (*TagMass*), and the negative logarithm of the confidence level of the four most displaced tracks in the jet being consistent with originating from the primary vertex (*JetBProbability*). The fit is performed using templates built from simulated events for b, c and light quarks. If a secondary vertex is reconstructed, both *TagMass* and *JetBProbability* are fit simultaneously, otherwise only *JetBProbability* was used. An example of fit in the data control region, for a typically populated bin, is shown in Fig. 2, with the b, c and light quark content of the third jet.

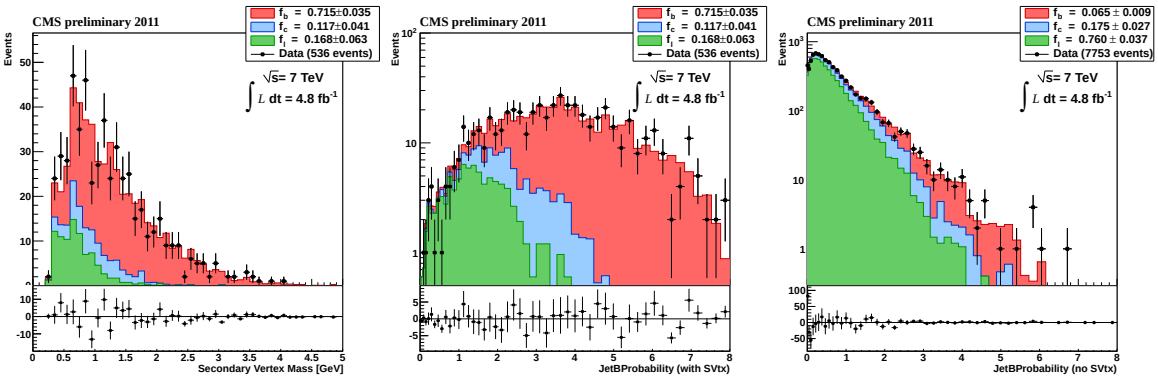

(a) *Tag Mass* (b) *JetBProbability* w/ *Tag Mass* (c) *JetBProbability* w/o *Tag Mass*

Figure 2: Example of a fit for one bin of the E_T, $|\eta|$ parametrization. The red, blue, and green histograms are respectively the templates for b, c, and light quarks. Dots represent data. Left and center: two-dimensional fit to *Tag Mass* and *JetBProbability*. Right: fit to *JetBProbability* only when the *Tag Mass* is not defined.

The results for the background prediction of the invariant mass distribution of the two leading jets is shown in Fig. 3, comparing the actual distribution in events with three b-tagged jets and the prediction. The plots are shown for the case of the low Higgs mass discriminator. The predictions are normalized to the number of events seen, and the original ratio of seen over predicted events is also shown, together with the result of a Kolmogorov-Smirnov test. The results are presented for data as well as for multijet MC simulation, as a closure test, for both control and signal region. The absolute normalization in the signal region will be described below.

An alternative data-driven method to estimate the background distribution makes use of a specialization of the generic type of algorithm called "nearest neighbor". In the case at hand, the scalar field to be estimated is the probability that an event pass the three b-tag selection. This is done by looking at the probability for events with similar kinematics in suitably-shaped hyperellipsoids in the multi-dimensional space of event and jet observables.

The method gives an independent prediction of the background shape and normalization in the signal region, and is used to get the systematics uncertainties for the predicted shape.

The test-events used are those passing all the preselection described above but with just the first jet b-tagged (bjj sample). The invariant-mass distribution for events passing the final selection is predicted starting from the sample of test-events failing the final selection and applying to each of them a weight accounting for the probability that all the 3 jets are b-tagged in the same event.

Among the test-events, N_T events with $Discr < 0.4$ are selected and used as a training sample. The probability for a test-event to pass the final selection is built by selecting a sample of $N_H = 100$ training events which are found the most *similar* (in the multi-dimensional sense discussed below) to the tested event, and computing the ratio of bbb and bjj event numbers inside that training sample.

The most similar events are chosen as the ones having the smallest multi-dimensional distance

$$D^2 = \sum_{i=1}^{n_V} w_i^2 \, (x_i - y_{\alpha i})^2 \tag{4}$$

where x_i are the n_V variables defining the test event and $y_{\alpha i}$ are the corresponding variables

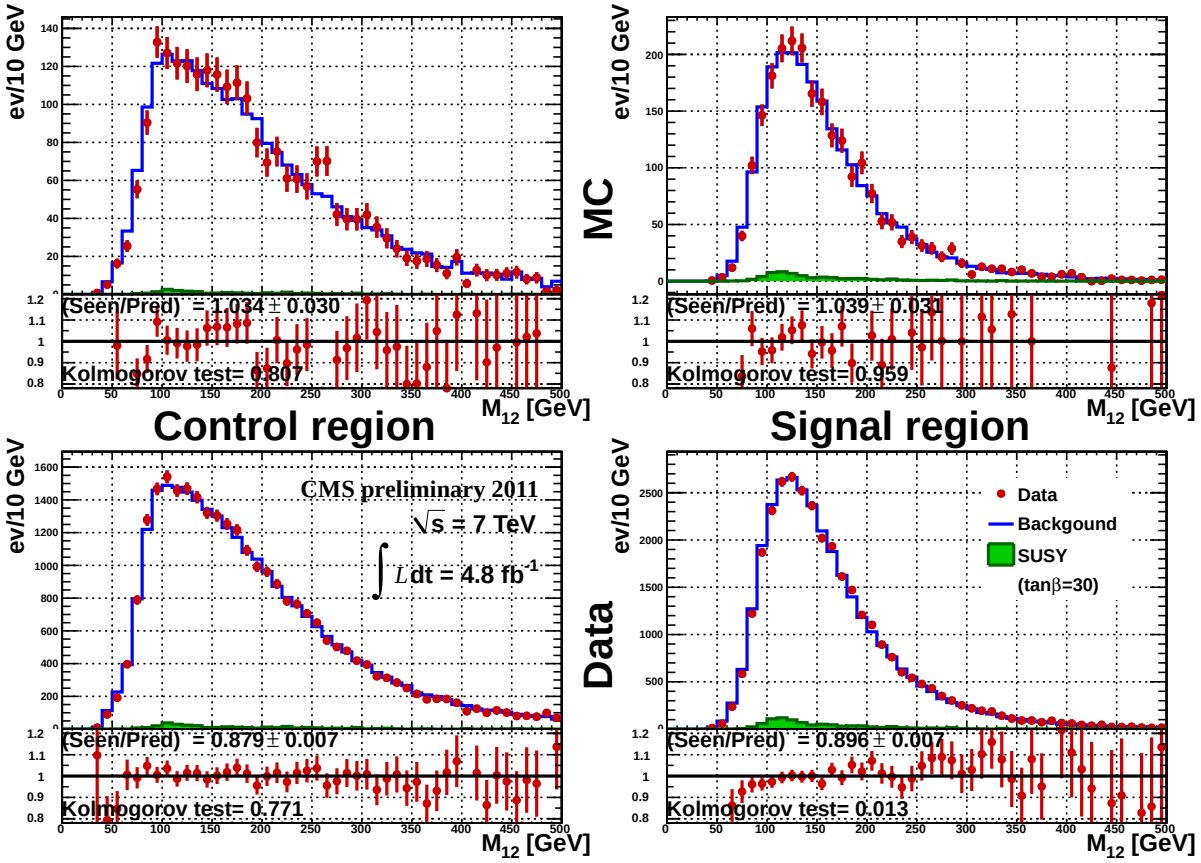

Figure 3: Invariant mass of the two leading jets, for MC and Data and for control and signal regions. Prediction (blue histogram), data (red dots) are overlaid. The prediction is normalized to data, and the normalization scale factor is also shown for each plot *(Seen/Pred)*. Also a hypothesis for a SUSY higgs signal at $M_h = 120\,\mathrm{GeV}/c^2$ with a production cross section corresponding to $\tan\beta = 30$ (green histogram) is overlaid.

in the training event α. The weights w_i account for the different dispersions of the variables and the different dependence of the b-tag probability on them. A numerical derivative of the probability for a test event to pass the final selection as a function of the variable x_i was taken as weight w_i.

The events having the transverse energies and pseudo-rapidities of the three leading jets near to the corresponding thresholds are handled in a special way. Those events are not centered in the hyper-ellipsoid, and the fraction of *bbb* events in the hyper-ellipsoid itself is not a good estimation of the probability for the test event to have all three jets b-tagged. This bias is cured by looking, for each test event, which variables among the transverse energies and pseudo-rapidities are near to the corresponding thresholds; a linear interpolation of the selection probability with those variables is performed and the result used to extrapolate the selection probability itself to the test event.

When all the energies and pseudo-rapidities in the tested event are not close to the above defined thresholds, the 3 b-tag probability for the test event was computed by a weighted ratio:

$$P = \frac{\sum_{\beta}^{bbb} 1/D_{\beta}^2}{\sum_{\alpha}^{bjj} 1/D_{\alpha}^2} \tag{5}$$

where in the numerator the sum runs over *bbb* events and in the denominator it runs over *bjj* events; D is the distance between the test event and the training event as defined in Eq. 4.

The results for the prediction of the invariant mass distribution of the two leading b-jets from the Hyperball and from the b-tagging matrix methods are compared in Fig. 4.

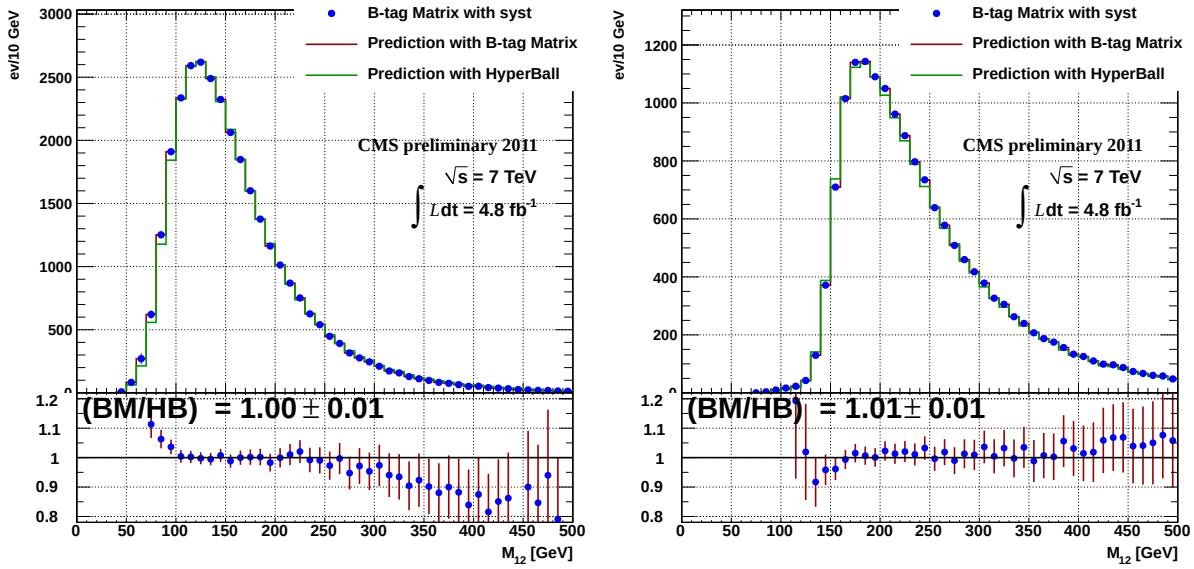

(a) Low Mass $M_H \leq 180\,\mathrm{GeV}/c^2$ (b) High Mass $M_H > 180\,\mathrm{GeV}/c^2$

Figure 4: Background predictions from the B-matrix and the Hyperball method compared for low mass region $M_H \leq 180\,\mathrm{GeV}/c^2$ (a) and high mass region $M_H > 180\,\mathrm{GeV}/c^2$ (b).

In the following of the analysis, the background prediction is taken from the b-tagging matrix method. The statistical uncertainty of the prediction is rescaled to take into account the difference observed between the two methods, which acts as a shape systematics.

6 Systematic uncertainties

Systematic uncertainties for this analysis can be separated in two categories: those affecting the signal yield and those related to the background prediction.

The main source of systematics of the event yield comes from uncertainties related to jets reconstruction and b-tagging. The second source is the trigger turn-on efficiency, given the rather low thresholds used in the event selection. Other sources include uncertainties on integrated luminosity, PDF modeling, and lepton-identification related ones.

The following uncertainties for the signal event yield are considered:

- **Trigger systematics**: the trigger turn-on applied to the signal is derived from data, along with its uncertainties which is mostly coming from the limited statistics of the pre-scaled trigger used as reference sample. This uncertainty is estimated to be $5-3\%$, depending to the Higgs mass;
- **b-tagging efficiency**: this contribution is studied in detail in a dedicated note [13] using a b-enriched sample from top decay as well as soft muon tag. The scale factor between MC and Data is included in the efficiency estimated from the MC and its error is used as a systematic uncertainty: 4% per jet, leading to 12% for three jets.

- **Jet Energy Scale**: the uncertainty in the Jet Energy Correction (JEC) is estimated by a standard procedure of scaling up and down the energy of all the jets in each event. Relative change in the amount of the events passing our offline selections is $^{+2.5}_{-3.1}\%$
- **Jet Energy Resolution**: to estimate the uncertainty from the Jet Energy Resolution (JER), the momenta of each generated jet is randomly adjusted according to a corresponding probability distribution for given p_T and η of the jet. An uncertainty of $\pm 1.9\%$ is associated to JER.
- **Muon momentum scale and resolution**: 0.2% and 0.6%;
- ***pdf* uncertainties**: estimated by reweighing signal MC by the uncertainties of the eigenvectors of covariance matrix of the original *pdf*. For $M_H = 120\,\mathrm{GeV}/c^2$: $^{+2.5}_{-2.7}\%$; for $M_H = 250\,\mathrm{GeV}/c^2$: $^{+4.7}_{-4.4}$;
- **Integrated luminosity**: 2.2% [11]

The background prediction is affected by two sources of systematic uncertainties: the shape of the prediction and its absolute normalization. As discussed in the previous section, the first is inferred by the comparison of the background predictions obtained with the b-tagging matrix and that obtained with the Hyperball method. The corresponding error scaling is included on bin-by-bin basis in the binned maximum likelihood fit to the distribution of the final observable (the invariant mass of the two leading b-tagged jets) discussed in next section.

The background normalization uncertainty has two components: the first is related to the level of agreement between the prediction and the actual *bbb* distribution in the data control region and the second is related to the extrapolation of this prediction from the control region to signal region. As seen in Fig. 3, the ratio between the prediction and the actual *bbb* distribution in the control region is fairly constant across the mass spectrum. Distributions for other kinematic variables not shown here display similar agreement. The normalization in the control region is 0.877 ± 0.007 for low mass and 0.885 ± 0.006 for high mass region. These numbers are used respectively as normalization factor for the prediction in the signal region and as systematic error on the background prediction ($0.8 - 0.7\%$). For the extrapolation from the control to the signal region, the MC simulation shown in Fig. 3 predicts a constant ratio between the prediction and data for the three b-jet event rate in the signal region. We compare the number of events in data over predicted in the signal and control region respectively: the ratio is 1.01 ± 0.042 and 1.02 ± 0.05 for low and high mass regions respectively. These values are used as a further correction to the normalization and set the uncertainty in the extrapolation from control and signal region.

7 Results and interpretation

In order to extract the possible contribution of a MSSM Higgs a binned likelihood fit to the invariant mass distribution of the leading two jets in the event is performed. Signal MC simulation predicts a peaked structure at a mass value around the Higgs mass.

Since there are two different discriminants, there are correspondingly two signal samples and two different background predictions. The predicted background is shown in Fig. 5 and 6 for the two mass ranges, respectively, together with the expected signal for different Higgs boson masses for $\tan\beta = 30$.

Throughout the analysis, the signal region corresponding to $Discr > 0.4$ was not studied. The efficiencies and background predictions are developed in an entirely blind way.

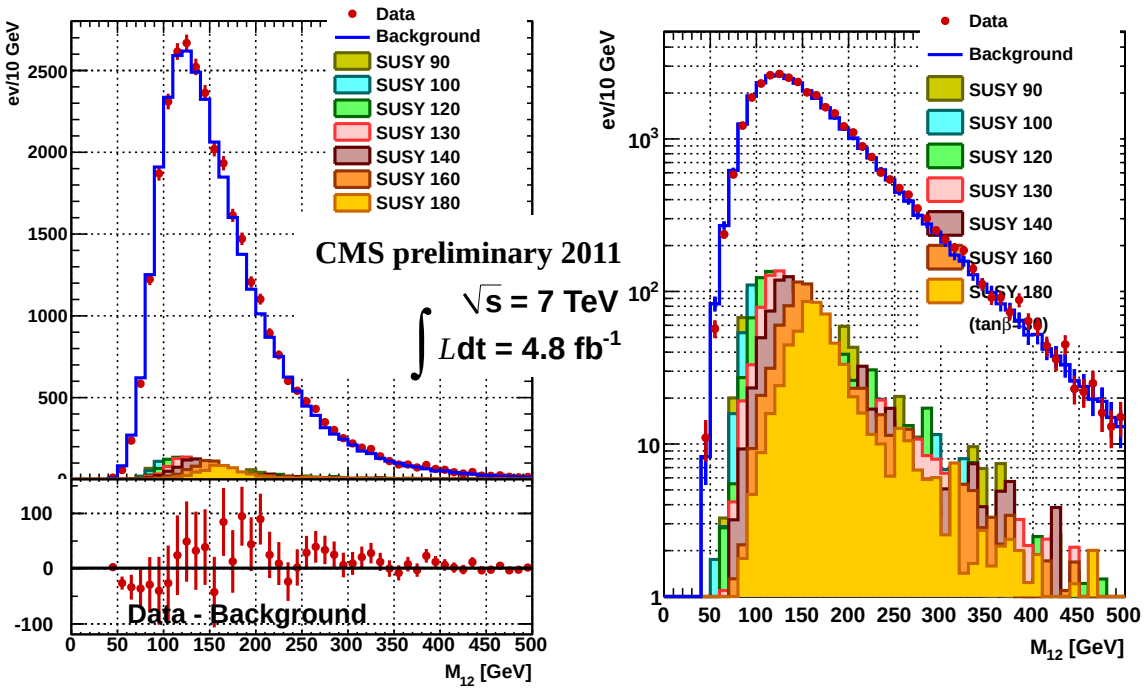

Figure 5: Data (red) and predicted background (blue) in the signal region, for low mass range ($M_H \leq 180\,\mathrm{GeV}/c^2$); the expected signal for different M_H and for $\tan\beta = 30$ is also plotted. Linear scale on the left, logarithmic on the right. The difference between data and predicted background is also shown.

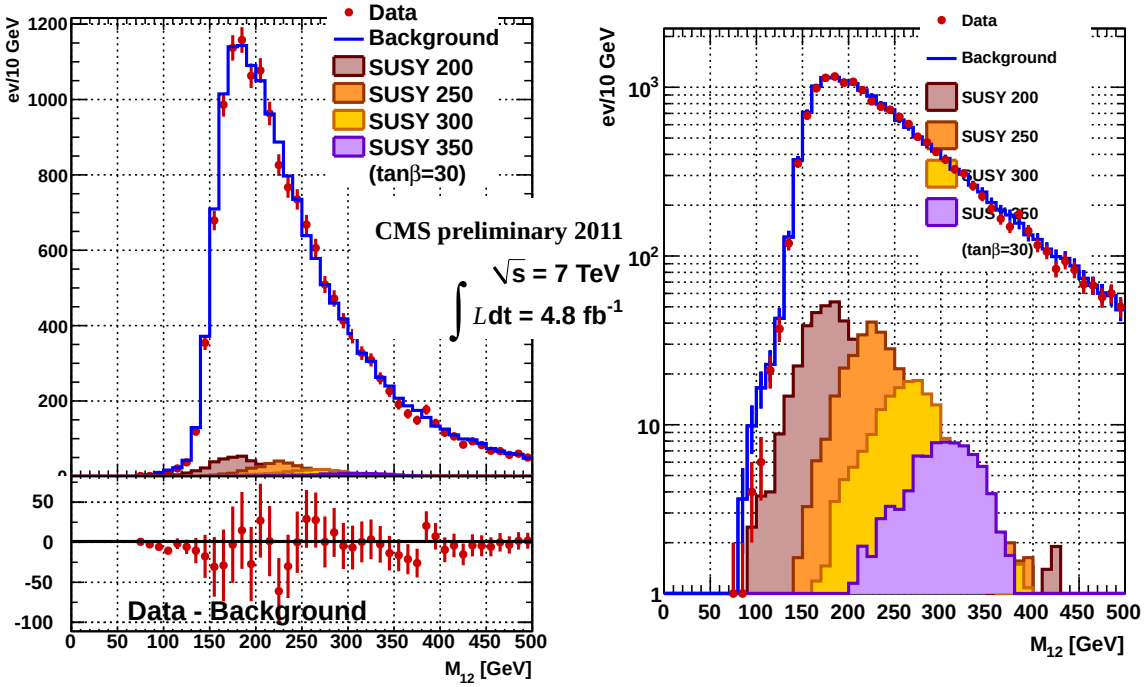

Figure 6: Data (red) and predicted background (blue) in the signal region, for low mass range ($M_H > 180\,\mathrm{GeV}/c^2$); the expected signal for different M_H and for $\tan\beta = 30$ is also plotted. Linear scale on the left, logarithmic on the right. The difference between data and predicted background is also shown.

The CL_s criterion is used to determine the 95% confidence-level limit on the signal contribution in the data, using the `RooStats` [17] package. Results are shown graphically in Fig. 7 in terms of cross section times branching ratio.

Figure 8 presents the results in the MSSM framework as a function of MSSM parameters $(M_A, \tan\beta)$, in the m_h^{max} scenario [18, 19], including all the statistical and systematical uncertainties.

In the MSSM m_h^{max} benchmark scenario, the definition of theory parameters are the following: $M_{SUSY} = 1\,\text{TeV}/c^2$; $X_t = 2M_{SUSY}$; $\mu = 200\,\text{GeV}/c^2$; $M_{\tilde{g}} = 800\,\text{GeV}/c^2$; $M_2 = 200\,\text{GeV}/c^2$; and $A_b = A_t$; $M_3 = 800\,\text{GeV}/c^2$. Here, M_{SUSY} denotes the common soft-SUSY-breaking squark mass of the third generation; $X_t = A_t - \mu/\tan\beta^2$ is the stop mixing parameter; A_t and A_b are the stop and sbottom trilinear couplings, respectively; μ is the Higgsino mass parameter; $M_{\tilde{g}}$ is the gluino mass; and M_2 is the SU(2)-gaugino mass parameter. The value of M_1 is fixed via the unification relation $M_1 = (5/3)M_2 \sin\theta_W / \cos\theta_W$. Finally, the 5 flavour schema is used.

The expected cross-section and branching ratio, in the MSSM framework, as calculated by bbh@nnlo [20] and FeynHiggs [21–24], respectively, are considered.

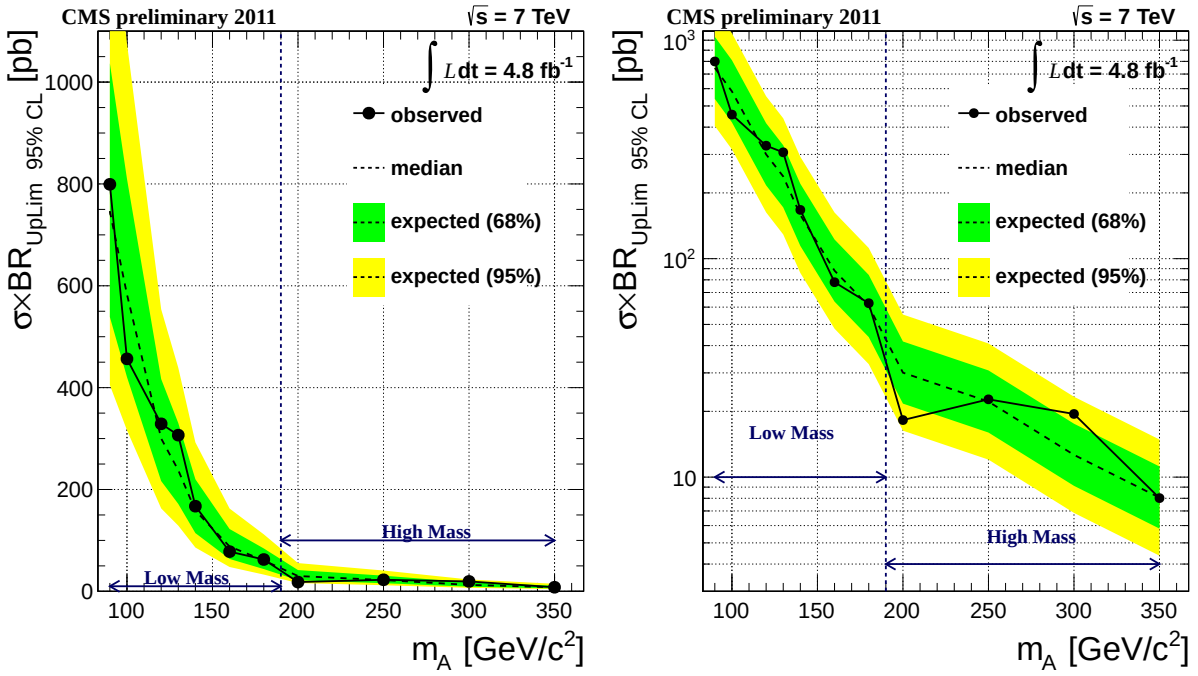

(a) Linear scale

(b) Logaritmic scale

Figure 7: Observed and expected upper limit for the cross section times branching ratio for 95% confidence level, with linear and logaritmic scale, with the inclusion of statistical and systematic uncertainties. The low and high mass regions are shown separately.

8 Conclusion

A search of neutral supersymmetric Higgs particles decaying into pairs of b-quarks, and produced in association with two further b-quarks, has been presented. The data were collected during 2011 by the CMS experiment at the LHC, corresponding to a total integrated luminosity of $4.8\,\text{fb}^{-1}$, with the use of a semileptonic trigger. Two data driven predictions of the large and dominating multijet QCD background have been developed.

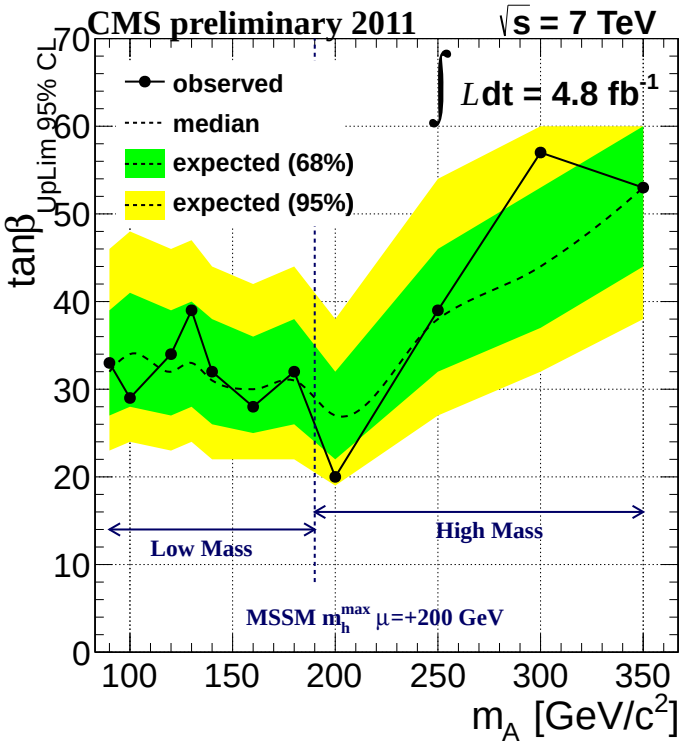

Figure 8: Observed and expected upper limit with 90% confidence level in the MSSM plane $(\tan\beta, M_A)$, including the statistical and systematical uncertainties, in the m_h^{max} benchmark scenario as defined in the text. The low and high mass regions are shown separately.

The data shows no significant excess with respect to the expected SM background, and a limit for Higgs cross section times branching ratio as a function of M_A is determined. These results are also interpreted in the framework of MSSM as a function of $(M_A, \tan\beta)$, in the m_h^{max} [18, 19] scenario, excluding a region of phase space previously unexplored for this final state.

Acknowledgements

We congratulate our colleagues in the CERN accelerator departments for the excellent performance of the LHC machine. We thank the technical and administrative staff at CERN and other CMS institutes, and acknowledge support from: FMSR (Austria); FNRS and FWO (Belgium); CNPq, CAPES, FAPERJ, and FAPESP (Brazil); MES (Bulgaria); CERN; CAS, MoST, and NSFC (China); COLCIENCIAS (Colombia); MSES (Croatia); RPF (Cyprus); MoER, SF0690030s09 and ERDF (Estonia); Academy of Finland, MEC, and HIP (Finland); CEA and CNRS/IN2P3 (France); BMBF, DFG, and HGF (Germany); GSRT (Greece); OTKA and NKTH (Hungary); DAE and DST (India); IPM (Iran); SFI (Ireland); INFN (Italy); NRF and WCU (Korea); LAS (Lithuania); CINVESTAV, CONACYT, SEP, and UASLP-FAI (Mexico); MSI (New Zealand); PAEC (Pakistan); MSHE and NSC (Poland); FCT (Portugal); JINR (Armenia, Belarus, Georgia, Ukraine, Uzbekistan); MON, RosAtom, RAS and RFBR (Russia); MSTD (Serbia); SEIDI and CPAN (Spain); Swiss Funding Agencies (Switzerland); NSC (Taipei); TUBITAK and TAEK (Turkey); STFC (United Kingdom); DOE and NSF (USA).

References

[1] CMS collaboration, "Combined results of searches for the standard model Higgs boson in pp collisions at $\sqrt{s}$ = 7 TeV.", doi:10.1016/j.physletb.2012.02.064.

[2] ATLAS Collaboration, "Combined search for the Standard Model Higgs boson using up to 4.9 fb^{-1} of pp collision data at $\sqrt{s}$ = 7 TeV with the ATLAS detector at the LHC.", *Phys. Lett. B* **710** (Feb, 2012) 49–66. 22 p, doi:10.1016/j.physletb.2012.02.044.

[3] H. Nilles, "Supersymmetry, supergravity and particle physics", *Physics Reports* **110** (1984), no. 12, 1 – 162, doi:10.1016/0370-1573(84)90008-5.

[4] CMS Collaboration, "Search for Neutral Higgs Bosons Decaying to Tau Pairs in pp Collisions at sqrts=7 TeV", *CMS-PAS-HIG-11-020* (2011).

[5] S. Schael et al. (The ALEPH, DELPHI, L3, and OPAL Collaborations), "Search for neutral MSSM Higgs bosons at LEP", *The European Physical Journal C - Particles and Fields* **47** (2006) 547–587.

[6] Tevatron New Phenomena & Higgs Working Group Collaboration, "Combined CDF and D0 Upper Limits on MSSM Higgs Boson Production in tau-tau Final States with up to 2.2 fb-1", arXiv:1003.3363.

[7] CDF Collaboration Collaboration, "Search for Higgs Bosons Produced in Association with *b*-quarks", *Phys.Rev.* **D85** (2012) 032005, arXiv:1106.4782. submitted to Phys. Rev. D.

[8] D0 Collaboration Collaboration, "Search for neutral Higgs bosons in the multi-b-jet topology in of collisions at", *Physics Letters B* **698** (2011), no. 2, 97 – 104, doi:10.1016/j.physletb.2011.02.062.

[9] CMS Collaboration, "MSSM Higgs production in association with b quarks - all hadronic", *CMS-PAS-HIG-12-026* (2012).

[10] CMS Collaboration, "The CMS experiment at the CERN LHC", *JINST* **3** (2008) S08004, doi:10.1088/1748-0221/3/08/S08004.

[11] CMS Collaboration, "Absolute Calibration of the Luminosity Measurement at CMS: Winter 2012 Update", *CMS-PAS-SMP-12-008* (2012).

[12] M. Cacciari, G. P. Salam, and G. Soyez, "The anti-k_t jet clustering algorithm", *JHEP* **04** (2008) 063, doi:10.1088/1126-6708/2008/04/063, arXiv:0802.1189.

[13] CMS Collaboration, "Performance of the b-jet identification in CMS", *CMS-PAS-BTV-11-001* (2011).

[14] J. Alwall, M. Herquet, F. Maltoni et al., "MadGraph 5 : Going Beyond", *JHEP* **1106** (2011) 128, arXiv:1106.0522.

[15] T. Sjstrand, S. Mrenna, and P. Skands, "PYTHIA 6.4 physics and manual", *Journal of High Energy Physics* **2006** (2006), no. 05, 026.

[16] S. Agostinelli, J. Allison, K. Amako et al., "Geant4a simulation toolkit", *Nuclear Instruments and Methods in Physics Research Section A: Accelerators, Spectrometers, Detectors and Associated Equipment* **506** (2003), no. 3, 250 – 303, doi:10.1016/S0168-9002(03)01368-8.

[17] L. Moneta, K. Belasco, K. Cranmer et al., "The RooStats Project", *PoS(ACAT2010)057* (2010).

[18] M. S. Carena et al., "MSSM Higgs boson searches at the Tevatron and the LHC: Impact of different benchmark scenarios", *Eur. Phys. J. C* **45** (2006) 797–814, doi:10.1140/epjc/s2005-02470-y.

[19] M. S. Carena et al., "Suggestions for benchmark scenarios for MSSM Higgs boson searches at hadron colliders", *Eur. Phys. J. C* **26** (2003) 601–607, doi:10.1140/epjc/s2002-01084-3.

[20] R. V. Harlander and W. B. Kilgore, "Higgs boson production in bottom quark fusion at next-to-next-to-leading order", *Phys. Rev. D* **68** (Jul, 2003) 013001, doi:10.1103/PhysRevD.68.013001.

[21] S. Heinemeyer, W. Hollik, and G. Weiglein, "FeynHiggs: a program for the calculation of the masses of the neutral CP-even Higgs bosons in the MSSM", *Computer Physics Communications* **124** (2000), no. 1, 76 – 89, doi:10.1016/S0010-4655(99)00364-1.

[22] S. Heinemeyer, W. Hollik, and G. Weiglein, "The masses of the neutral CP-even Higgs bosons in the MSSM: Accurate analysis at the two-loop level", *The European Physical Journal C - Particles and Fields* **9** (1999) 343–366.

[23] G. Degrassi, S. Heinemeyer, W. Hollik et al., "Towards high-precision predictions for the MSSM Higgs sector", *The European Physical Journal C - Particles and Fields* **28** (2003) 133–143.

[24] M. Frank, T. Hahn, S. Heinemeyer et al., "The Higgs boson masses and mixings of the complex MSSM in the Feynman-diagrammatic approach", *Journal of High Energy Physics* **2007** (2007), no. 02, 047.